CHAPTER 4

Investigations on the structural characteristics that seed the aggregation of $A\beta_{1-42}$ peptide: Insights from molecular dynamics simulations

Investigations on the structural characteristics that seed the aggregation of $A\beta_{1-42}$ peptide: Insights from molecular dynamics simulations

4.1. Abstract:

$A\beta_{1-42}$ peptide is known to be the primary component of the amyloid plaques found in the brain of patients suffering from AD. Extensive research has been done in the past with respect to $A\beta_{1-42}$ peptide and its involvement in AD. However, the initial seed structure responsible for the $A\beta_{1-42}$ peptide aggregation and the mechanism remains unclear. This may be chiefly attributed to the poor understanding of the processes involved in the $A\beta_{1-42}$ peptide misfolding and aggregation. Furthermore, the flexibility and the aggregation propensity involved in the $A\beta_{1-42}$ monomer, challenges the experimental and theoretical techniques to characterize the seed structure that drive the misfolding and the subsequent aberrant aggregation. In this Chapter, we have employed all atoms fully unrestrained folding MD simulation to identify the structural characteristics of the probable seed structure of $A\beta_{1-42}$ peptide responsible for the aggregation. The initial linear structure of the $A\beta_{1-42}$ peptide for the simulation was built from its amino acid sequence using leap module of AMBER. From our study, we followed the secondary structural development in $A\beta_{1-42}$ peptide starting from its initial linear structure to its folded 3-D structure. We observed the $A\beta_{1-42}$ peptide to sample diverse conformations which are rich in β-sheets and are stabilized by hydrogen bonding and other non-bonding interactions. The findings of this study shall be helpful in understanding the initial stage of $A\beta_{1-42}$ peptide aggregation process and can be applicable for the development of therapeutics to cure AD at an early stage.

4.2. Introduction:

As discussed in Chapter 2, $A\beta_{1-42}$ peptide which is the primary component of extracellular senile plaques in AD exists normally in α-helical state; later misfold into a β-sheet conformation to form the pathogenic amyloid plaques [4, 5]. There were several works [67-70, 184-186] that have been carried out but till now the physiological and pathological characteristics of $A\beta_{1-42}$ peptide in AD is not well understood. Thus it is necessary to understand the molecular details of the toxic intermediates in the early stage of $A\beta_{1-42}$ peptide aggregation as this will be helpful for the rational design of therapeutics to prevent AD. Despite a high degree of sophistication, the experimental

techniques have not yet been done in $A\beta_{1-42}$ peptide to provide an atomistic level of insight into the initial conformational transitions of $A\beta_{1-42}$ peptide and the subsequent folding that leads to misfolded aggregation prone structures.

In this study, we have outlined the folding pattern of $A\beta_{1-42}$ peptide from its initial primary structure (amino acid sequence) throwing light on the sequence of events and the type of interactions that eventually lead to the aggregation prone structure of the $A\beta_{1-42}$ peptide. So, we have carried out the unrestrained folding simulation [187] for $A\beta_{1-42}$ peptide to characterize the folding pattern, early sequential conformational transitions leading to the aggregation prone structure. We have initiated the peptide folding simulation of $A\beta_{1-42}$ peptide using its amino acid sequence with an extended initial conformation built by the LEaP module of AMBER12 [164] and this has allowed us to find and study a large variety of conformers of $A\beta_{1-42}$ peptide starting from an extended initial conformation to the subsequent folding conformations. Apart from that, the structural organization of the $A\beta_{1-42}$ peptide was studied at higher temperatures to analyze their impact on generation of β-strands in $A\beta_{1-42}$ peptide.

4.3. Materials & Methods:

4.3.1. $A\beta_{1-42}$ peptide folding simulation:

We have performed MD simulation with the AMBER12 software package [164] on the $A\beta_{1-42}$ peptide utilizing the AMBER ff99SB force field [188] parameters for proteins. We built the linear structure of $A\beta_{1-42}$ peptide from its amino acid sequence using the LEaP module of AMBER12. The usage of an explicit solvent model may result in errors due to variations in the heat capacity of water as well as conformational effects due to confined aqueous volume and therefore we have utilized Generalized Born (GB) implicit solvent model [189].

To remove the unfavorable contacts in the peptide structure, the resultant structure was subjected to energy minimization using 500 steps of steepest descent and another 500 steps of conjugate gradient method. The minimized structure was then subjected to 100 ps of MD using 2 fs time step for integration. During the MD simulation, the system was gradually heated from 0 to 300 K and ensured slow relaxation of the built initial structure.

The bonds to the hydrogen atoms were constrained using the SHAKE algorithm [167]. Subsequently MD was performed under constant pressure-temperature conditions (NPT) with temperature regulation achieved using Berendsen weak coupling method

[168] (0.5ps time constant for heat bath coupling and 0.2 ps pressure relaxation time) and calculated electrostatic forces using the particle-mesh Ewald procedure (PME) [190]. This heating dynamics was followed by another 20 ps of equilibration step. To ensure equilibration, the potential, kinetic and total energy, RMSD, pressure, density and temperature of the system was monitored. Finally for the analysis of structures and properties we carried out 80 ns of NPT MD using a heat bath coupling time constant of 1 ps. Following the MD run, trajectory files were obtained which were later used for analysis using cpptraj [191]. After the MD run, the Visual Molecular Dynamics (VMD) package [192] was used for visualization of the 3-D structure of the peptide.

4.3.2. $A\beta_{1-42}$ mutant (Lys 28 to Pro 28) peptide folding simulation:

Using the protocol mentioned in section 4.3.1 we built the 3-D structure for the mutant of $A\beta_{1-42}$ peptide from the amino acid sequence. In the mutant amino acid sequence, we used Proline (β-sheet breaker) at the position 28 in the place of Lysine. We then carried out the MD simulation to study the conformational dynamics and folding pattern as described in section 4.3.1.

4.3.3. $A\beta_{1-42}$ peptide simulation at higher temperature:

The equilibrated $A\beta_{1-42}$ peptide structure after equilibration as described in section 3.3.1 was used to carry out MD simulation studies at six different temperatures (325 K, 350 K, 400 K, 425 K, 450 K, and 500 K). We carried out 10 ns of NPT MD for each temperature. After the MD run, the VMD package [192] was used for visualization of the 3-D structure of the molecule.

4.4. Results & Discussions:

4.4.1. Conformational stability of $A\beta_{1-42}$ peptide from the simulation:

Secondary structural changes of the extracellular $A\beta_{1-42}$ peptide from its native α-helix to random coils and β-strands, resulting in its aggregation prone structure is believed to be the major risk factor in AD. In this study, we have predicted the probable seed structure of $A\beta_{1-42}$ peptide that triggers the aggregation by constructing the $A\beta_{1-42}$ peptide from its initial amino acid sequences, using *ab initio* unrestrained folding simulation. We first assessed the stability and quality of the conformations sampled out during the simulation of $A\beta_{1-42}$ peptide, by analyzing the temperature as shown in **Figure 4.1.A** and potential energy as a function of time (**Figure 4.1.B**), and observed that the system was successfully equilibrated.

Subsequently, we have investigated the relative conformational stabilities of the $A\beta_{1-42}$ peptide by measuring the RMSD with reference to the equilibrated structure. We found that the backbone RMSDs of the peptide deviates up to 10 ns and then the structure was converged and attained almost stable conformation as shown in **Figure 4.2.A**. The RMSD plot confirmed that the $A\beta_{1-42}$ peptide structure underwent rapid structural changes and finally reached equilibration after 10 ns of the simulation period. The stability of the peptide was found to depend on the formation of β-sheets. As the β-sheets appeared in the peptide after 10 ns and the structure was rendered stable. This is in conformity to the work that has been reported previously on the stability of the peptide structure with respect to β-sheets [185].

We have also isolated the $A\beta_{1-42}$ conformer having the lowest potential energy from the production trajectory. Then we carried out RMSD analysis (**Figure 4.2.B**) for the structures in the trajectory with the lowest potential energy conformer as the reference structure. In Figure **4.2.B**, we have showed the backbone RMSD relative to this lowest potential energy conformer during the course of the same simulation from Figure **4.1.B**. A clear correlation between potential energy and RMSD could be seen from Figure **4.2.B** and **4.1.B**. We also observed the potential energy plateau in Figure **4.1.B** at the simulation time, as the structural convergence occurred in Figure **4.2.B**. In Figure **4.2.B**, we also noticed that the plateau has been maintained from 22 ns to 80 ns of the simulation time period. So the folded structure of $A\beta_{1-42}$ peptide formed after 22 ns can be said to be relatively stable and also have undergone folding to a significant extent. Thus, even though our system does not seem to have reached a completely stable structure as seen from the RMSD analysis, it was found to undergo folding to attain a structure that showed stability for a time period exceeding 60 ns.

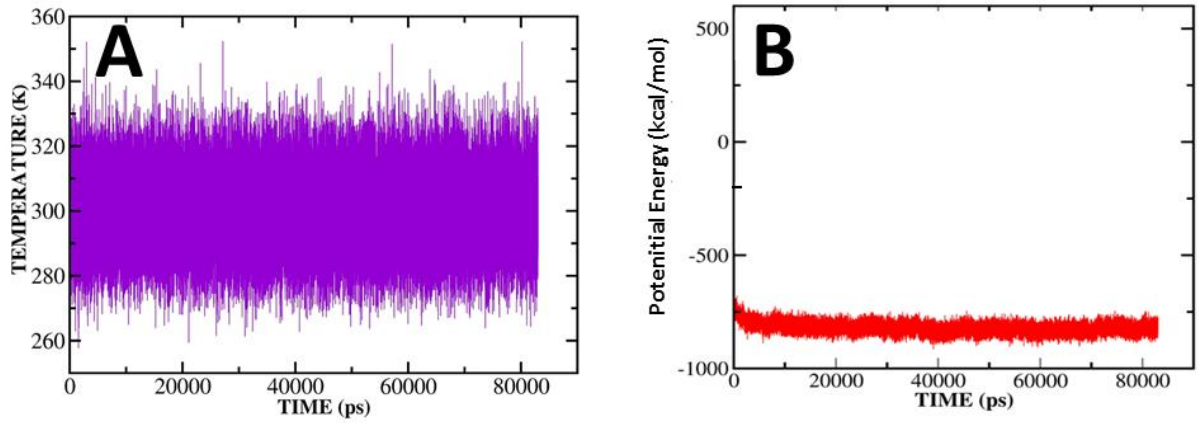

Figure 4.1. *A) Temperature vs time course of simulation period; B) Potential Energy vs time course of simulation period for* $A\beta_{1\text{-}42}$ *peptide structure.*

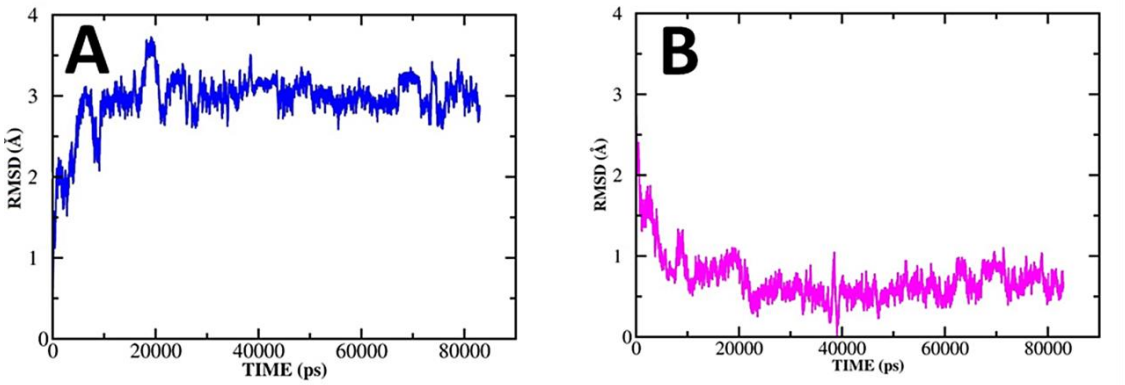

Figure 4.2. *Backbone RMSD vs time course of simulation period for the A)* $A\beta_{1\text{-}42}$ *peptide with the equilibrated structure as the reference structure; B)* $A\beta_{1\text{-}42}$ *peptide with lowest potential energy conformer as the reference structure.*

Furthermore, to investigate the local deformability in the $A\beta_{1-42}$ peptide chain, the B-factor values for the backbone atoms were analyzed against their residue number. The B-factors values for the backbone C-α atom in $A\beta_{1-42}$ peptide chain are shown in **Figure 4.3**. The data clearly shows higher B-factor value of the backbone atoms of the residues in the regions 17-25, 30-37 & 40-42. These regions in $A\beta_{1-42}$ peptide chain are thus considered to exhibit higher flexibility thus accounting for frequent change in the secondary structures leading to the formation of diverse conformers.

To examine the compactness of the peptide during the simulation time course, Rg was measured. Rg is a measure of the mass-weighted spatial distribution of the atoms in a peptide molecule and a rough measure for its compactness. The value of Rg depends on the total number of amino acids constituting a protein. **Figure 4.4** shows the Rg of $A\beta_{1-42}$ peptide chain backbone as a function of time. It is observed that, the peptide oscillated to a greater degree before 10 ns, during the course of simulation followed by less fluctuation after 10 ns. This is mainly due to secondary structural changes and rigidity. In the time course of simulation, the disordered regions might have underwent extensive conformational changes and thus caused higher fluctuation in Rg. Also the hydrophobic core present in the peptide might have lost its compressibility leading to much variation in Rg during the first 10 ns. It seems that the structural convergence and folding occurred after 10 ns from the simulation being initiated.

4.4.2. Secondary structure characteristics of $A\beta_{1-42}$ peptide:

Using the DSSP tool [183] we plotted the secondary structure transitions of each residue in the $A\beta_{1-42}$ peptide as a function of simulation time (as shown in **Figure 4.5**). From the **Figure 4.5**, we can see that, most of the residues in $A\beta_{1-42}$ peptide have shown secondary structural transitions from helix to coils and turns. At the same time, we also observed certain regions (Residue index: 18-20, 28-35 and 39-42) to show transitions from helix to β-sheet.

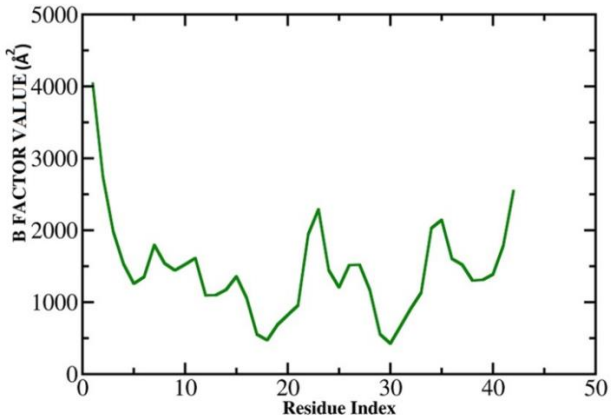

Figure 4.3. *B-factor values of C-α atoms as a function of residue number is shown for $A\beta_{1-42}$ peptide.*

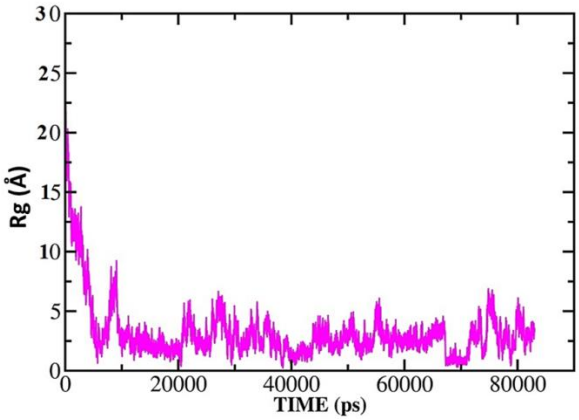

Figure 4.4. *Radius of gyration as a function of time course of simulation for the $A\beta_{1-42}$ peptide.*

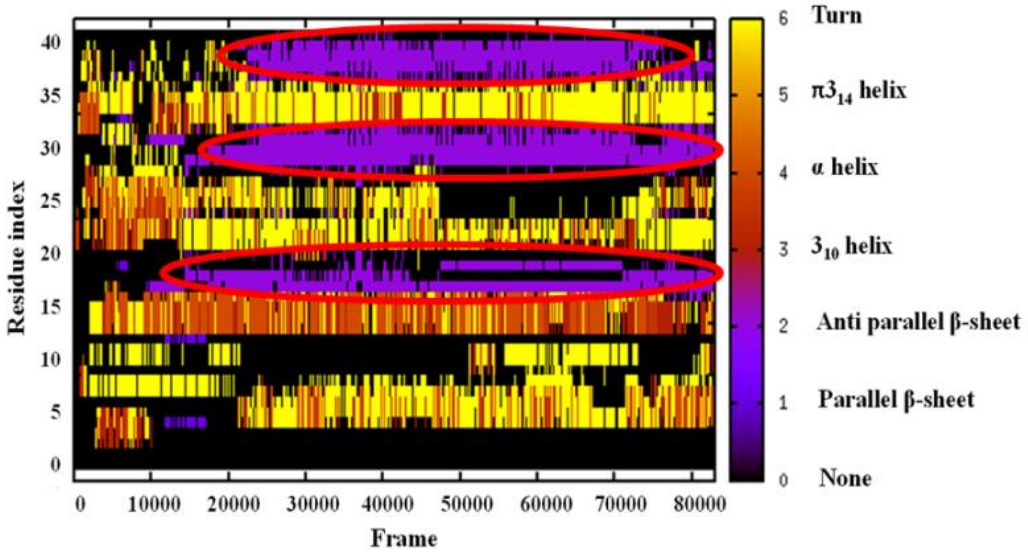

Figure 4.5. *Secondary structure assignment per residue for the $A\beta_{1-42}$ peptide conformer during the time course of simulation period. (The encircled portion in red shows the appearance of β-strands in $A\beta_{1-42}$ peptide).*

Additionally, we have also determined the probable secondary structure and the score corresponding to each of the residues in $A\beta_{1-42}$ peptide and plot is shown in Figure **4.6**. From Figure **4.6**, we observed that peak in red color which corresponds to anti-parallel β-sheets are predominant in the regions 18-20, 29-35 and in the C-terminus of the $A\beta_{1-42}$ peptide. The probability score plot was noticed to have correlation with the secondary structural evolution. In addition, we also saw that the residues in the region 18-21, 30-35 and 39-42 favored β-structures with probability score of 0.6-0.8. These data are consistent with prior studies that have suggested β-strand propensities in the Ile31-Val36 and Val39-Ile41 as well as a turn characters in $A\beta_{1-42}$ peptide [193].

Residues Val18-Phe20 and Val39-Ile41 indicate a bias towards φ dihedrals which is a characteristic of β-strands in these regions [194, 195]. However, the $A\beta_{1-42}$ peptide conformational ensemble from the folding pattern has not been elucidated yet, from which we can trace out the plausible seed structure responsible for aggregation, the main focus of our study. Here we have constructed the $A\beta_{1-42}$ peptide from the sequence itself via *ab initio* approach and studied the folding pattern wherein we observed the secondary structural transitions to β-sheets. The results also indicated that the loop region (residue index: 5 to 13) showed less flexibility with minor variations between the helix and sheet occurrences during the simulations.

We also took snapshots of the $A\beta_{1-42}$ peptide at different time intervals of the simulation period that are shown in **Figure 4.7**. From the **Figure 4.7**, we were able to observe β-sheet development during the course of simulation period. From the snapshots, we also observed that the β-strands initially developed at two regions, 30-32 and 39-42 and then at a turn region in the residue index 32-38. From the earlier reports, we could see that the stabilization of turn like structure at 25-29 was due to hydrophobic interaction between Val24 and Lys28 and electrostatic interactions between Glu22 or Asp23 and Lys28 [196]. We also observed the appearance of β-strands at region 18-20 and characteristic turn at the segment within the region 21-29 that drives the $A\beta_{1-42}$ peptide to fold in a particular pattern, which is consistent with the previous work done by Roychaudhari *et al*. [197]. The earlier reports indicated that segment 21-30 forms a turn that act as a monomer folding nucleus which seemed to be favored by the salt bridge between residues Asp23 and Lys28. Importance of turn in folding and stability of protein has also been reported by Jihun Lee and his group [198] where they studied the

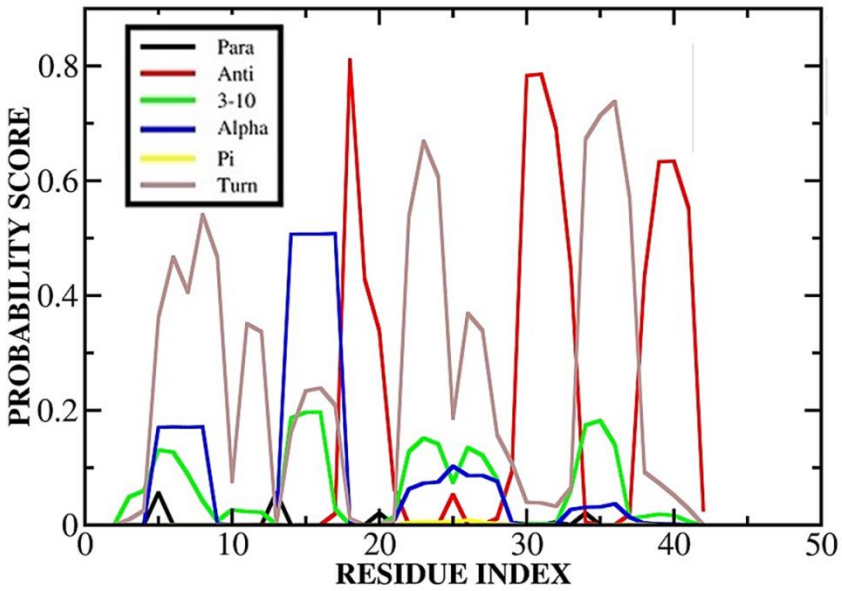

Figure 4.6. *Probability score of secondary structure assignment per residue for the average structure of $A\beta_{1-42}$ peptide during the time course of simulation period.*

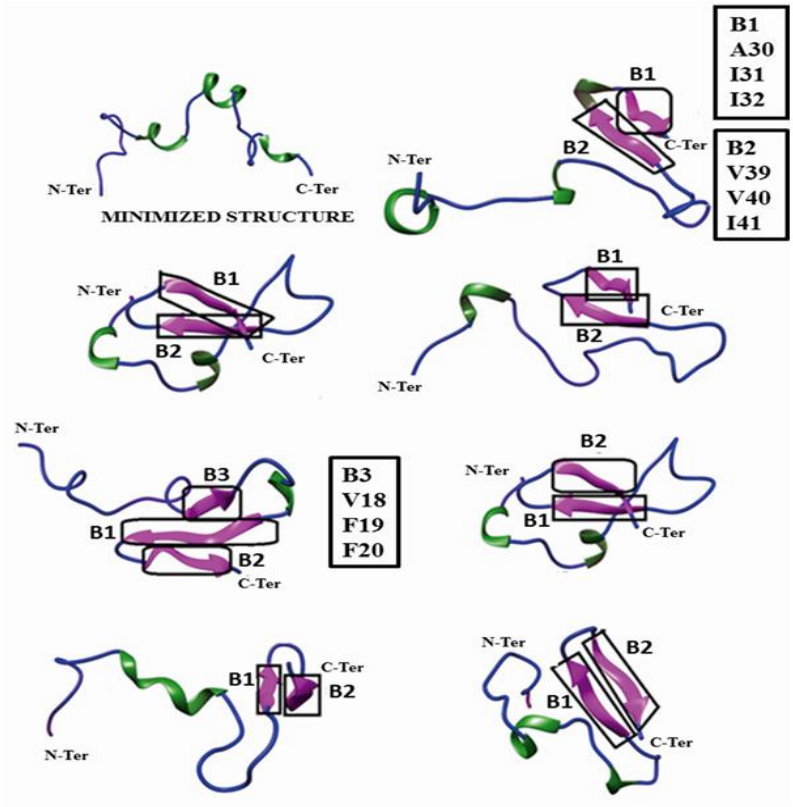

Figure 4.7. *Snapshots of $A\beta_{1-42}$ peptide wild type at 300 K during the time course of simulation period.*

type I β-turns with a combination of Asx mutation in human fibroblast growth factor-1, and determined their effects on structure, stability, and folding. Their study showed that the Asx residues in the turn motif with a consensus sequence of Asx-Pro-Asx-Gly made a substantial contribution to the overall stability of the protein, wherein Asx could be Asp or Asn. Although the turn that we observe at the region 21-29 was not found to exhibit the consensus sequence, Asp and Asn at position 23 & 27 were respectively observed. Akira Morimoto and his group [199] also highlighted the turn at position 33-39 that stabilize the $A\beta_{1-42}$ peptide by forming a circular structure and another turn at position around 22 -23 to organize the $A\beta_{1-42}$ fibrils. The turn encompassing residues 35 & 36 is stated to be important for the alignment of the strands. The loops formed at the N-terminal end exhibits a tight *van der Waals* as these regions were found to display complementarity of molecular surfaces.

We have carried out simulations to further assess the relevance of the data by comparison of $A\beta_{1-42}$ peptide with the mutant $A\beta_{1-42}$ peptide where Lysine at the 28th amino acid position was replaced with Proline. We observed a few helices in the structure at residues ranging from 6-12, 22-25, and 28-36 but no β-strands (**Figure 4.8**). Because of the absence of salt bridge that normally existed in wild type between Asp23-Lys28, the mutant structure lacked the characteristic folding pattern and the stabilization of the monomer structure that was imparted by the salt bridge.

Overall, we observed that $A\beta_{1-42}$ peptide was enriched in β-sheets particularly at the three regions (30-32, 39-42, 18-21) and underwent a typical folding at around 22 ns which was stabilized by the salt bridge. From the snapshots of (**Figure 4.7**), we could see some of the hydrophobic residues (Val18, Phe19, Phe20, Ala30, Ile31, Ile32, Val39, Val40 and Ile41) were involved in forming the β-strands. These residues in the β-strands enhance the stabilization of the β-sheets formed later by long range hydrophobic contacts in addition to interaction with each other by forming cross-strand main chain H-bonds. Moreover, with the number of hydrophobic contacts substantially higher in comparison to α-helix, sheets are more likely to result in the exposure of hydrophobic residues under destabilizing factors such as mutation and/or misfolding. To prevent the exposure of these hydrophobic residues, the rich transient β-strands and hairpins at the C-terminal of $A\beta_{1-42}$ peptide might entropically favor the peptide aggregation by forming dimers, then tetramer and finally oligomers via formation of hydrophobic core by the hydrophobic residues. The importance of hydrophobic interactions between the

β-sheets in amyloid fibrils was also point out by the *in situ* AFM of $A\beta_{1-42}$ peptide aggregation upon hydrophilic mica or hydrophobic graphite [200]. However, at very high temperature, we observed that the structure of $A\beta_{1-42}$ peptide contained only loops and coils and no β-strands (**Figure 4.9**).

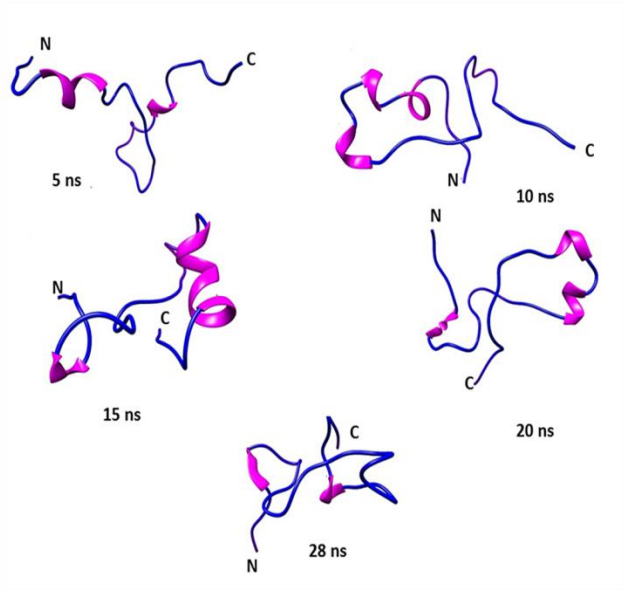

Figure 4.8. *Snapshots of $A\beta_{1-42}$ peptide mutant at 300K during the time course of simulation period.*

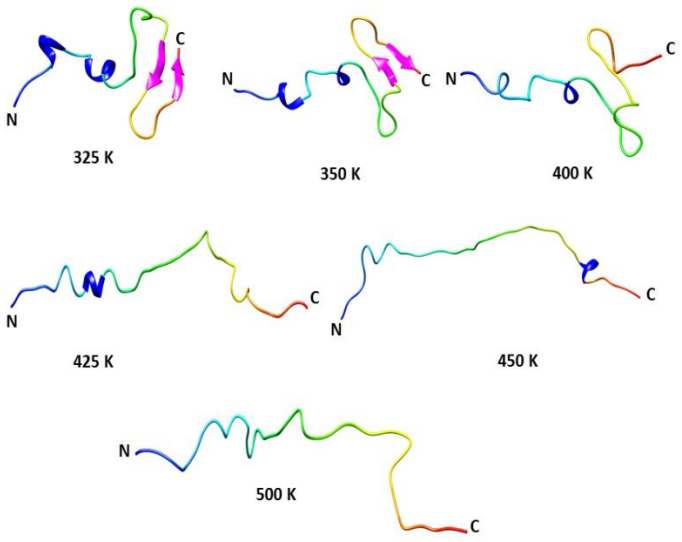

Figure 4.9. *Snapshots of intermediates and final configuration of MD simulations of $A\beta_{1-42}$ peptide structure at higher temperatures.*

Other factors including protein amino acid sequence, solvent pH, temperature, ionic strength, concentration of the protein, the presence of cosolutes viz. denaturants including urea, chaotropes/kosmotropes including osmolytes and ligands that interact selectively with native/non-native protein conformations or the aggregated form, and the presence/ absence of various molecular chaperones may also favor the aggregation process [201].

4.5. Conclusions:

In this work, we have demonstrated the structural features of the probable seed structure of $A\beta_{1-42}$ peptide from the MD simulation study. We have charted down the development of secondary structure in $A\beta_{1-42}$ peptide right from its initial linear structure that has been built from its amino acid sequence to the formation of stable 3-D structure. During the time course of our simulation, we found the formation of extensive β-strands at specific regions (30-32; 39-42). These regions have been highlighted for the aggregation prone area in many of the earlier studies. Not surprisingly, we notice the seed structure to be highly rich in β-strands at the C-terminal end which has been reported to be structured. We also observed the characteristic turn for the motif in the region 32-38 that may be considered to play significant role in alignment of the strands. In addition our findings from the simulation indicated β-strands at region 18-20 and characteristics of a turn at the segment within the region 21-29 that actually result in the folding of $A\beta_{1-42}$ peptide monomer. The residues encompassing the β-strands are found to be hydrophobic in nature and thereby may invoke the stabilization of the sheets which will form later by long range hydrophobic contacts and backbone hydrogen bonds. Our findings from the folding simulation in this study as a whole dictate the probable characteristic features of seed structure of $A\beta_{1-42}$ peptide that initiate aggregation. We hope that this study will expand the scope of understanding the initiatives for Alzheimer's amyloid aggregation process and can be applicable for the development of therapeutics to cure AD, which can be validated through *in vitro* and *in vivo* biological tests.